

## Background

The geometric analysis and simulation was conducted by assuming a prolate shape of all amyloidogenic peptides. The simulation concluded that a spiking-out orientation of a prolate was required in order to reproduce the extracted peptide coverage ratio, Q. The involvement of a secondary layer was suggested; this secondary layer was considered to be due to the networking of the peptides. Both Ab1-40 and b2m are considered to have a partial charge (especially d+) distribution centering around the prolate axis. The  $\alpha$ -syn, on the other hand, possesses a distorted charge distribution. For relatively lower Q (i.e.,  $Q < 0.56$ ), a prolate was assumed to conduct a gyration motion, maintaining the spiking-out orientation in order to fill in the unoccupied space with a tilting angle of approximately 25°.

## Calculation Hypothesis:

### #1 Peptide Prolate



**Figure 1.** A schematic diagram of sequences for three amyloidogenic peptides a)  $A\beta_{1-40}$ , b)  $\alpha$ -syn, and c)  $\beta$ 2m were assumed to have a prolate shape.

### #2 Orientation

We focus on the orientation of the peptide by assuming the peptide shape as a simple prolate. The orientation of this prolate can be roughly considered to be two ways either lay down or spiking out over the spherical surface of nano-gold colloidal surface.

As the first approximation, the lay-down orientation can be more stable and can possess higher interaction between a peptide and gold colloidal surface.

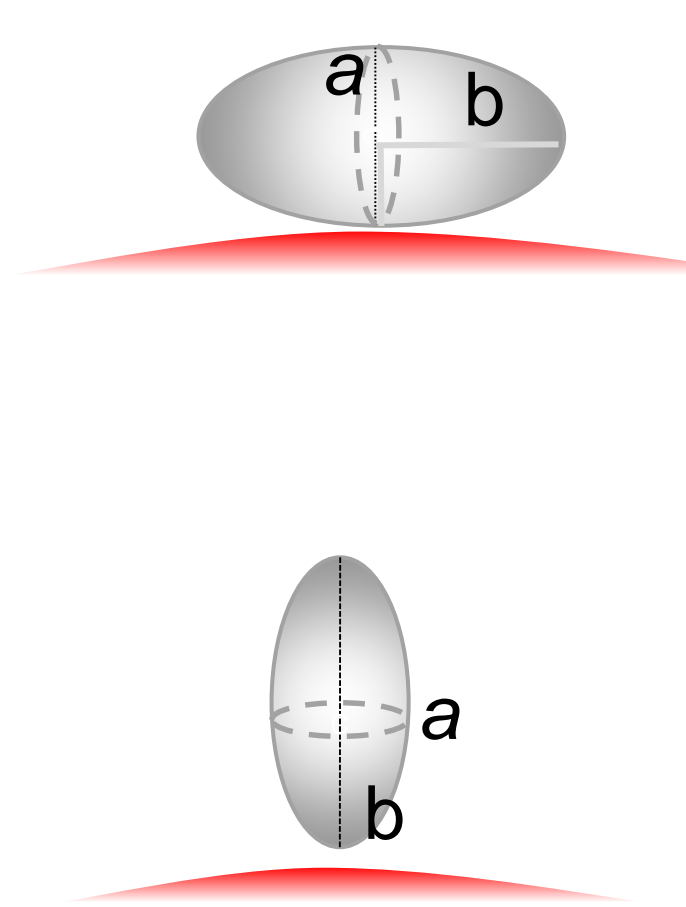


**Figure 2.** The horizontal and vertical orientation of the prolate were calculated.

### Calculation for First Layer:

**Figure 3.** A schematic procedure simulating the coverage ratio of a peptide over a gold-nano colloidal sphere.

- [1] A conceptual sketch indicating that  $A\beta_{1-40}$  was simplified as a prolate top and the expected orientation of a prolate to cover the gold colloidal surface.
- [2] A procedure of counting the adsorption point along axial axis;  $n_{ax}$ . The detailed procedure of extracting the  $n_{ax}$  for the case of gold colloid of  $d = 30 \text{ nm}$  ( $d = 30.7 \text{ nm}$ ).

$$l_b = \sqrt{r^2 - b^2} \quad l_{max} = \left\lfloor \frac{a+l_b}{2a} \right\rfloor$$

$$n_i = \left\lfloor \frac{2\pi+(r+a)}{2b} \right\rfloor, r_i = \sqrt{r^2 - l_i^2}, l_i = \frac{l_b - a}{l_{max}} \times i, \quad n_{eq} = \left\lfloor \frac{2\pi+(r+a)}{2b} \right\rfloor$$

- [3] A procedure of counting the adsorption point along equatorial axis;  $n_{eq}$ . The detailed procedure of extracting the  $n_{eq}$  for the case of gold colloid of  $d = 30 \text{ nm}$  ( $d = 30.7 \text{ nm}$ ).

$$n_i = \left\lfloor \frac{2\pi+(r+a)}{2b} \right\rfloor \quad r_i = \sqrt{r^2 - l_i^2}, l_i = \frac{l_b - a}{l_{max}} \times i$$

- [4] A procedure of counting total number of adsorption points ( $n_{total}$ ).

$$\Theta = \frac{A_{prolate}}{A_{sphere}} \times n_{tot}$$

$$A_{prolate} = \pi ab \quad A_{sphere} = 4\pi(r+a)^2$$

- [5] A schematic sketch of the imaginary surface area covering the prolate over the nano gold colloid with a radius,  $r$ . The concept used to calculate the coverage fraction, ( $\Theta$ ).

### Calculation for Second Layer

**Figure 4.** A schematic procedure simulating the 2<sup>nd</sup> layer coverage ratio of a peptide over a nano-gold colloidal sphere. Zz

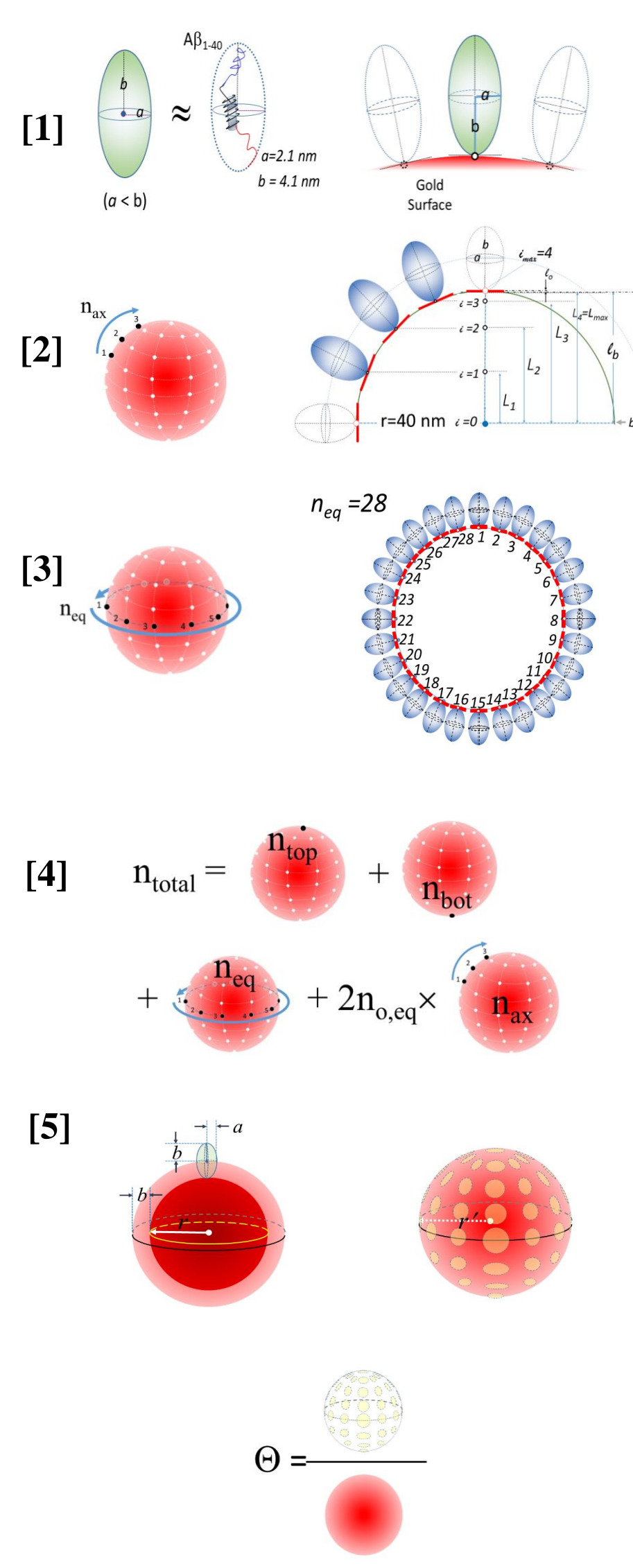
- [1]' A procedure of counting the adsorption point along axial axis;  $n_{o,ax}$  over the 2<sup>nd</sup> layer. The detailed procedure of extracting the  $n_{o,ax}$  for the case of gold colloid of  $d = 30 \text{ nm}$  ( $d = 30.7 \text{ nm}$ ).
- [2]' A procedure of counting the adsorption point along equatorial axis;  $n_{o,eq}$  over the 2<sup>nd</sup> layer. The detailed procedure of extracting the  $n_{o,eq}$  for the case of gold colloids with a  $d = 30 \text{ nm}$  ( $d = 30.7 \text{ nm}$ ).

- [3]' A procedure of counting the total number of adsorption points at the 2<sup>nd</sup> layer ( $n_{o,total}$ ).

- [4]' A schematic sketch of imaginary surface area covering the prolate over the nano-gold colloid with a radius,  $r$ . The concept of calculating the coverage fraction,  $\Theta'$ . When the total coverage ratio for the 1<sup>st</sup> and 2<sup>nd</sup> layer was calculated, the overlapped area between both layers was counted once.

$$\Theta' = \frac{A' \times n_{total}}{A_{sphere}} \quad \Theta_{total} = \Theta_{total(1st)} + \gamma \Theta_{total(2nd)}$$

- [5]' An overall schematic sketch of either optimizing  $a$  and  $b$  length of unit prolate in a single layer model for each gold size, as well as the empirical parameter. The combination optimizing  $a$  and  $b$  length, were utilized to reproduce the obtained  $\Theta$  for all gold colloidal sizes under all three amyloidogenic peptides coated over their surfaces.



## Results

**Table 1.** The summary of calculated axial length of prolate ( $a$  and  $b$ ) for a)  $A\beta_{1-40}$ , b)  $\alpha$ -syn, and c)  $\beta$ 2m. The extracted  $\Theta$ ,  $\Theta_{obs}$ , was reproduced as  $\Theta_{total}$  by combining  $\Theta$  calculated for the 1<sup>st</sup> layer ( $\Theta_{1,cal}$ ) and for the 2<sup>nd</sup> layer ( $\Theta_{2,cal}$ ) with the ratio of 2<sup>nd</sup>  $\Theta_{cal}$  ( $\gamma$  ( $\Theta_{2,cal}$ )) used to reproduce the extracted  $\Theta$ ,  $\Theta_{obs}$ . The number of attached prolates over the 1<sup>st</sup> layer was shown under  $n_1$ .

a)  $A\beta_{1-40}$

| Gold, d (nm) | Gold, d (nm) | a (nm) | b (nm) | $n_1$ | $\Theta_{1,cal}$ | $\Theta_{2,cal}$ | $\gamma$ ( $\Theta_{2,cal}$ ) | $\Theta_{obs}$ | $\Theta_{total}$ |
|--------------|--------------|--------|--------|-------|------------------|------------------|-------------------------------|----------------|------------------|
| 10           | 9.8 (10)     | 1.4    | 2.2    | 39    | 0.3791           | 0.5881           | 0.4425                        | 0.6393         | 0.6393           |
| 15           | 15.2 (15)    | 1.4    | 2.2    | 91    | 0.4643           | 0.6530           | 0.5687                        | 0.8357         | 0.8357           |
| 20           | 19.7 (11)    | 1.4    | 2.2    | 111   | 0.3746           | 0.7228           | 0.5116                        | 0.7443         | 0.7443           |
| 30           | 30.7 (13)    | 1.4    | 2.2    | 287   | 0.4566           | 0.7911           | 0.3027                        | 0.6961         | 0.6961           |
| 40           | 40.6 (11)    | 1.4    | 2.2    | 528   | 0.5111           | 0.8449           | 0.4112                        | 0.8585         | 0.8585           |
| 50           | 51.5 (40)    | 1.4    | 2.2    | 854   | 0.5357           | 0.8697           | 0.0877                        | 0.6119         | 0.6119           |
| 60           | 60.0 (10)    | 1.4    | 2.2    | 1212  | 0.5728           | 0.8461           | 0.0570                        | 0.6210         | 0.6210           |
| 80           | 80.0 (10)    | 1.4    | 2.2    | 2038  | 0.5608           | 0.8957           | 0.2321                        | 0.7687         | 0.7687           |
| 100          | 99.5 (13)    | 0.905  | 3.72   | 597   | 0.1958           | 0.1847           | 0.0023                        | 0.1962         | 0.1962           |

b)  $\alpha$ -syn

| Gold, d (nm) | Gold, d (nm) | a (nm) | b (nm) | $n_1$ | $\Theta_{1,cal}$ | $\Theta_{2,cal}$ | $\gamma$ ( $\Theta_{2,cal}$ ) | $\Theta_{obs}$ | $\Theta_{total}$ |
|--------------|--------------|--------|--------|-------|------------------|------------------|-------------------------------|----------------|------------------|
| 10           | 9.8 (10)     | 4.6    | 7.4    | 10    | 0.3497           | 0.5099           | 0.5292                        | 0.6195         | 0.6195           |
| 15           | 15.2 (15)    | 4.6    | 7.4    | 12    | 0.2821           | 0.4600           | 1.1470                        | 0.8098         | 0.8098           |
| 20           | 19.7 (11)    | 4.6    | 7.4    | 13    | 0.2311           | 0.6876           | 0.7128                        | 0.7213         | 0.7213           |
| 30           | 30.7 (13)    | 4.6    | 7.4    | 39    | 0.3966           | 0.6096           | 0.4525                        | 0.6745         | 0.6745           |
| 40           | 40.6 (11)    | 4.6    | 7.4    | 48    | 0.3309           | 0.7303           | 0.6860                        | 0.8319         | 0.8319           |
| 50           | 51.5 (40)    | 4.6    | 7.4    | 92    | 0.4429           | 0.6588           | 0.2278                        | 0.5929         | 0.5929           |
| 60           | 60.0 (10)    | 4.6    | 7.4    | 105   | 0.3971           | 0.7714           | 0.2653                        | 0.6018         | 0.6018           |
| 80           | 80.0 (10)    | 4.6    | 7.4    | 186   | 0.4379           | 0.7919           | 0.3876                        | 0.7448         | 0.7448           |
| 100          | 99.5 (13)    | 1.4    | 7.4    | 190   | 0.1881           | 0.2056           | 0.0100                        | 0.1902         | 0.1902           |

c)  $\beta$ 2m

| Gold, d (nm) | Gold, d (nm) | a (nm) | b (nm) | $n_1$ | $\Theta_{1,cal}$ | $\Theta_{2,cal}$ | $\gamma$ ( $\Theta_{2,cal}$ ) | $\Theta_{obs}$ | $\Theta_{total}$ |
|--------------|--------------|--------|--------|-------|------------------|------------------|-------------------------------|----------------|------------------|
| 10           | 9.8 (10)     | 2.5    | 4.6    | 10    | 0.4710           | 0.2414           | 0.0026                        | 0.4716         | 0.4716           |
| 15           | 15.2 (15)    | 2.5    | 4.6    | 17    | 0.1785           | 0.6403           | 0.8987                        | 0.7540         | 0.7540           |
| 20           | 19.7 (11)    | 2.71   | 6.41   | 16    | 0.4405           | 0.2687           | 0.0017                        | 0.4409         | 0.4409           |
| 30           | 30.7 (13)    | 2.5    | 4.6    | 101   | 0.3965           | 0.8526           | 0.4600                        | 0.7887         | 0.7887           |
| 40           | 40.6 (11)    | 2.5    | 4.6    | 175   | 0.4410           | 0.8851           | 0.3460                        | 0.7473         | 0.7473           |
| 50           | 51.5 (40)    | 2.5    | 4.6    | 276   | 0.4682           | 0.9061           | 0.3081                        | 0.7473         | 0.7473           |
| 60           | 60.0 (10)    | 2.98   | 4.25   | 88    | 0.4709           | 0.4832           | 0.0055                        | 0.4735         | 0.4735           |
| 80           | 80.0 (10)    | 2.5    | 4.6    | 666   | 0.5231           | 0.9843           | 0.3676                        | 0.8850         | 0.8850           |
| 100          | 99.5 (13)    | 2.98   | 4.25   | 1025  | 0.5479           | 0.99973          | 0.4424                        | 0.9902         | 0.9902           |

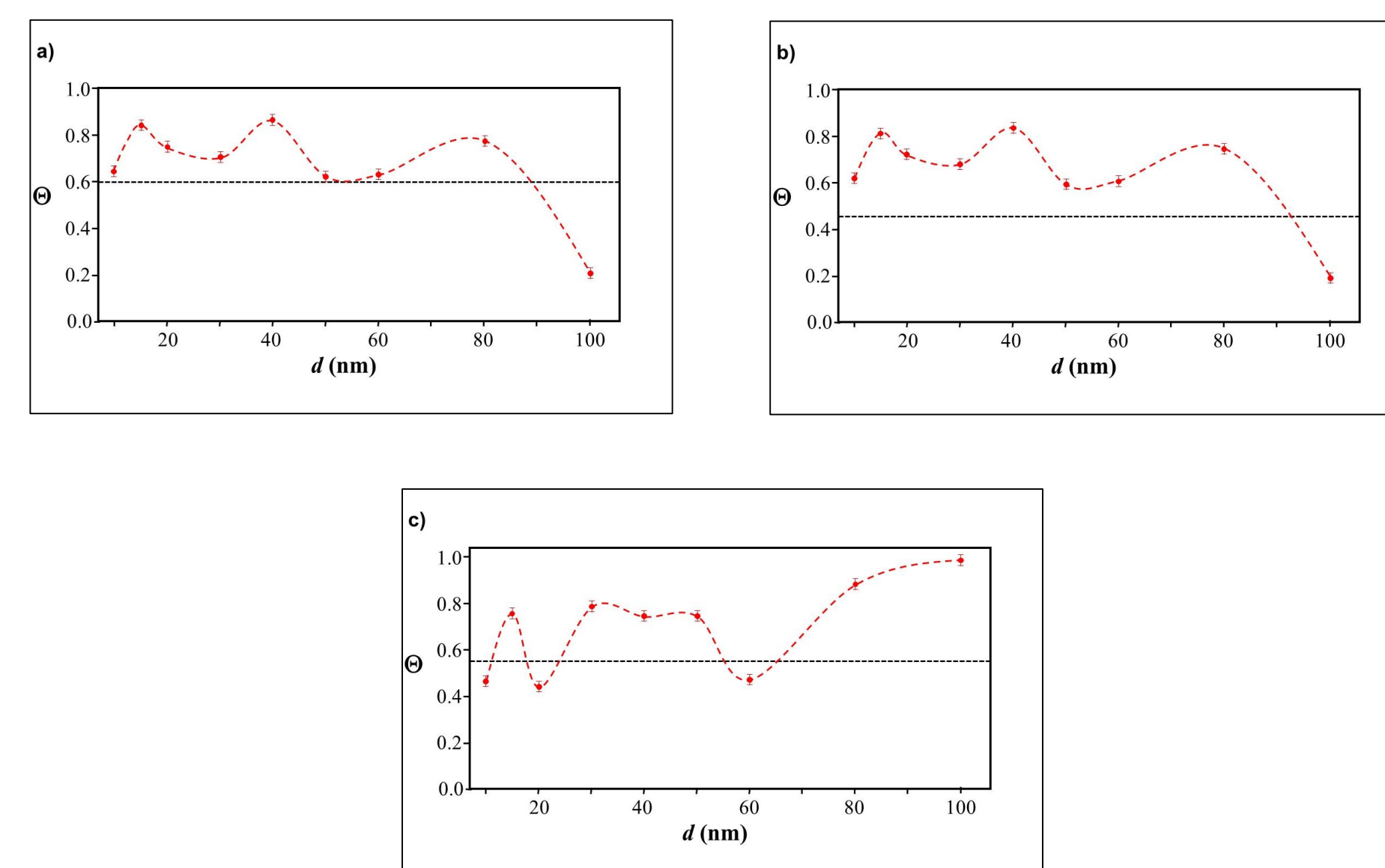


**Figure 5.** A plot for experimentally obtained  $\Theta$  for a)  $A\beta_{1-40}$ , b)  $\alpha$ -synuclein, and c)  $\beta$ 2m. A blue solid line composed of a collection of simulated values described in the text. The dotted line shows an upper limit of the  $\Theta$  value obtained by a single layer model.

## References

K. Yokoyama "Nano Size Dependent Properties of Colloidal Surfaces" Book Chapter in "Colloids: Classification, Properties and Applications" Edited by P. C. Ray (Nova Science Publishing) ISBN# 978-1-62081-128-3, pp. 25-58 (2012)  
 K Yokoyama (editor) controlling a reversible self assembly path by nanoscale metal surface. -study of fibrillogenesis of Alzheimer's disease  
 Kelly et al. 2005. How to study proteins by circular dichroism. *Biochimica et Biophysica Acta*. 119-139

## Acknowledgements

The Geneseo Foundation is greatly appreciated for their generous contribution towards this project.

## Discussion

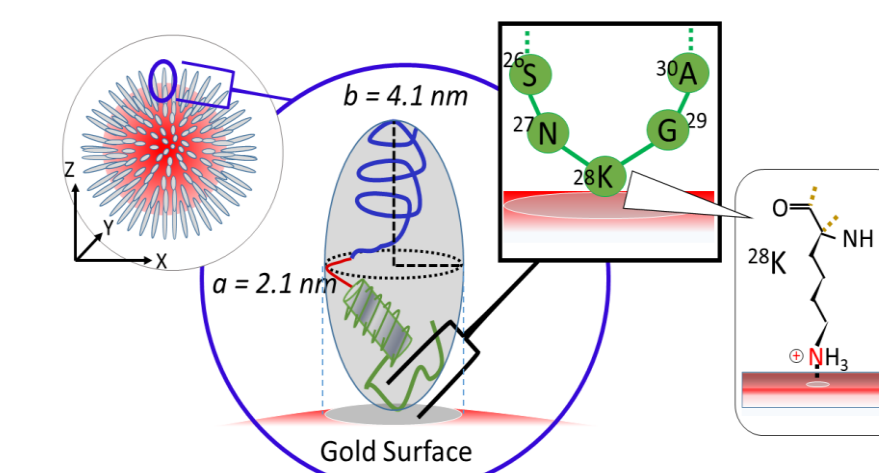


**Figure 6.** The proposed attachment structure of  $A\beta_{1-40}$  over the surface of a gold colloidal particle.

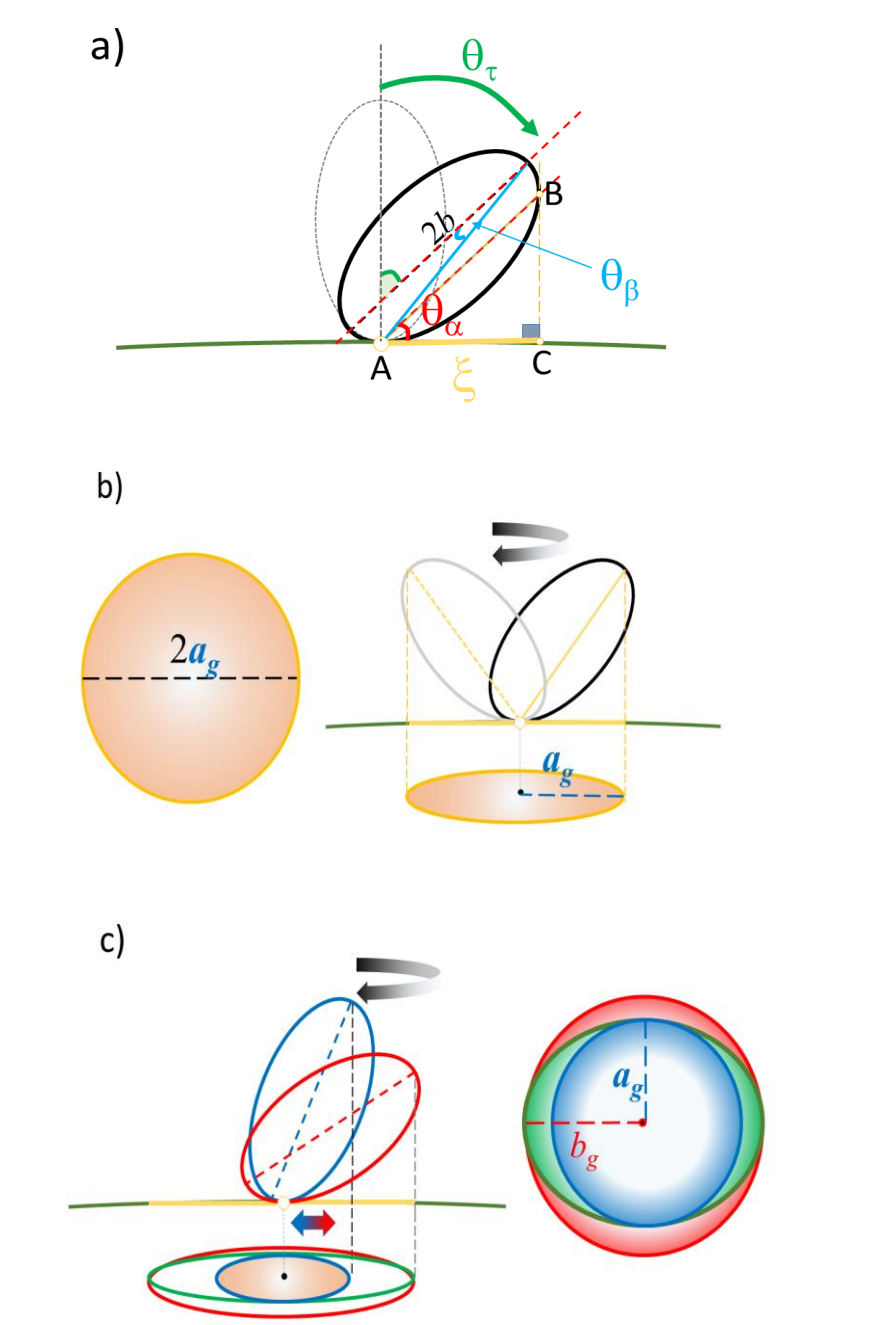


**Figure 7.** A sketch of the side view of a rotating prolate. a) The tilting of a prolate over the nano-gold surface and approximation for radius ( $L$ ) of the circular plane over the nano surface. b) A rotational motion of a prolate with a fixed contacting point, resulting in a circular occupied space over the surface. c) A gyration motion of a prolate with a movable contacting point, resulting in an oval occupied space over the surface.

**Table 2.** The list of extracted tilting angles ( $\theta_\alpha$  and  $\theta_\beta$ ) for the lower coverage for a)  $A\beta_{1-40}$ , b)  $\alpha$ -syn, and c)  $\beta$ 2m.

| a) $A\beta_{1-40}$ |         | b) $\alpha$ -syn |         | c) $\beta$ 2m |         |         |
|--------------------|---------|------------------|---------|---------------|---------|---------|
| d                  | d       | d                | d       | d             | d       | d       |
| 99.5               | 99.5    | 7.400            | 7.400   | 9.80          | 19.7    | 60.0    |
| 2.200              | 2.200   | 7.400            | 7.400   | 4.6           | 4.6     | 4.6     |
| 3.720              | 3.720   | 7.400            | 7.400   | 4.03          | 6.41    | 5.40    |
| 57.721°            | 57.721° | 30.000°          | 30.000° | 25.980°       | 44.166° | 35.942° |
| 32.279°            | 32.279° | 60.000°          | 60.000° | 64.020°       | 45.834° | 54.058° |
| 0.155°             | 0.155°  | 0.000°           | 0.000°  | 0.354°        | 0.064°  | 0.326°  |
| 0.905              | 0.905   | 1.40             | 1.40    | 2.70          | 2.73    | 4.80    |
| 11.870°            | 11.870° | 5.428°           | 5.428°  | 17.067°       | 17.262° | 31.449° |
| 78.130°            | 78.130° | 81.247°          | 81.247° | 72.933°       | 72.738° | 58.551° |
| 0.565°             | 0.565°  | 0.127°           | 0.127°  | 0.508°        | 0.234°  | 0.060°  |

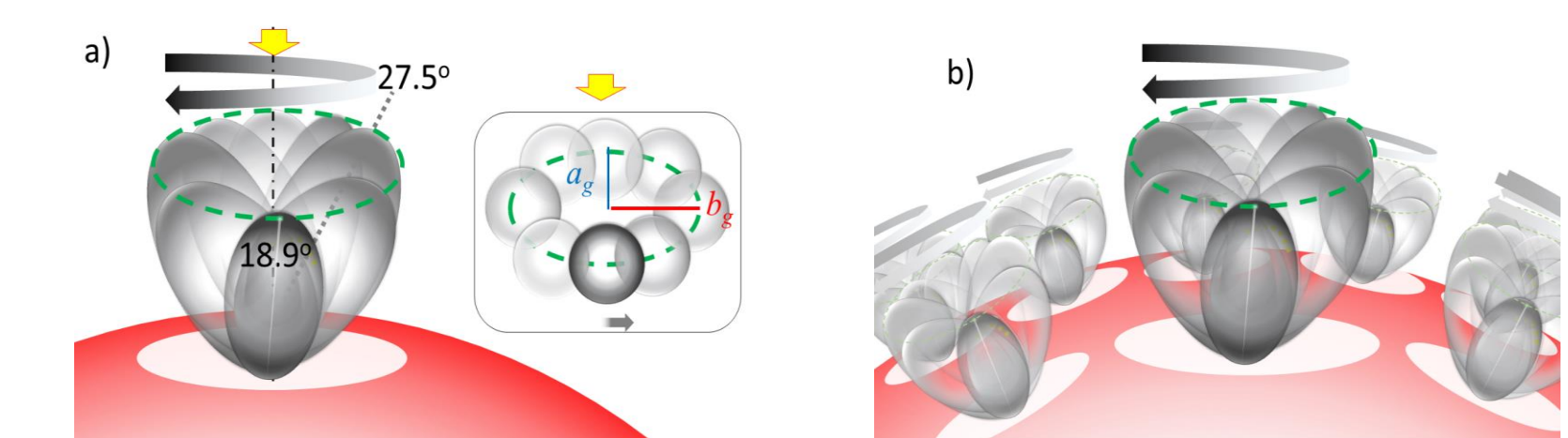


**Figure 8.** a) The sketch showing the gyration motion of a prolate ( $a = 2.5 \text{ nm}$  and  $b = 4.6 \text{ nm}$ ) representing  $\beta$ 2m over a gold nano-particle with a diameter of  $d = 60 \text{ nm}$ , where the prolate major axis tilts between 27.5° and 18.9° as it rotates over the surface. It results in an oval occupied space with  $a = 2.98 \text{ nm}$  and  $b = 4.25 \text{ nm}$ . (See Table 3) b) The sketch of a gyrating prolate over the nano-gold particle surface.

## Conclusions

The surface properties of nano-gold colloidal surfaces due to adsorption of amyloidogenic peptides were successfully monitored and characterized by observing the response of spectroscopic features as a function of an external pH change. This surface property change was found to be linearly correlated with the coverage ratio of the peptide,  $\Theta$ . With the simplification of the space occupied by a peptide into a prolate, the  $\Theta$  was extracted through a simplified tessellation logic applied for a sphere. The simulation suggested that a prolate needs to have a spiking-out orientation with prolate axial length of ( $a, b$ ) = (1.4 nm, 2.2 nm) for  $A\beta_{1-40}$ , ( $a, b$ ) = (4.6 nm, 7.4 nm) for  $\alpha$ -syn, and ( $a, b$ ) = (2.5 nm, 4.6 nm) for  $\beta$ 2m. The segment possesses a  $\delta^+$  that was considered to be highly used when  $A\beta_{1-40}$  and  $\beta$ 2m each interacted with nano-gold colloidal surface. This possesses a distribution of centering around the prolate axis. On the other hand, the  $\delta^+$  of  $\alpha$ -syn was used to interact between each monomer, and the charge distribution was spread around with a distortion, resulting in a high exposure for the counter acting monomer.